BALLISTIC SURFACE DIFFUSION

Y. MA and L.D. MARKS

Materials Research Center, Northwestern University, Evanston, Illinois 60208, USA

The ballistic diffusion of the surface atoms after collisions with high-energy electrons is simulated numerically. The time for the ballistic diffusions of a monolayer under the bombardment of the high energy electron is estimated semi-quantitatively.

1. Introduction

There is a growing interest in the use of electron microscopy to study surfaces whether by reflection [1–4], profile [5–8] or by straight transmission [9–12], in addition to the established interest in reflection high-energy electron diffraction (RHEED). Unfortunately, like all other techniques, the electron beam both probes and changes the structure of a surface. In particular, two unwanted processes can occur, enhanced thermal surface diffusion due simply to electron beam heating and athermal surface diffusion by either an electronic mechanism [13] or by direct knock-on of a surface atom. Except for highly insulating materials, experiments (in transmission) have shown that the temperature rise due to beam heating is small, of the order of 10 K [14,15], and can therefore be neglected. For athermal processes, the incoming electrons can cause electronic transitions which become converted into atomic motion leading to either preferential desorption of one species [16–18] or surface diffusion [13]; electron-stimulated desorption of diffusion for which various models have been proposed [19–22]. However, knock-on mechanisms for surface diffusion have not been investigated in detail. In this paper we report the results of calculations for this process, athermal ballistic surface diffusion due to Rutherford scattering.

2. Model and analysis

Ballistic surface diffusion can be divided into two steps: the initial scattering of the electrons which provides an impulse to the target atom and the actual diffusion of the atom (after the electron has left). The former is a collision process and finishes in a very short time, about 10^{-19} s. The latter is the dynamical motion of the scattering atoms in the surface potential, and takes place with the more leisurely time scale of thermal vibrations, i.e. 10^{-12} s. Our approach here is to consider first the diffusion problem for a range of different vectors for the initial atom momentum, and then later to tie in the results from these calculations of the probability that the atom will defuse or be sputtered with calculations of the actual initial momentum of the target (which is a function of the beam energy and direction relative to the surface).

To model the dynamical motion of surface atoms, we used a Lennard-Jones potential, with 6 rows and 20 atoms in each row (figs. 1a and 1b), taking for our parameters those of gold [23]. (A Lennard-Jones potential was used solely as a pragmatic choice to make the problem tractable.) The blackened atoms in both figures are the atoms whose classical trajectories were numerically integrated. The case shown in fig. 1a models an adatom, whilst fig. 1b models a flat surface, and in
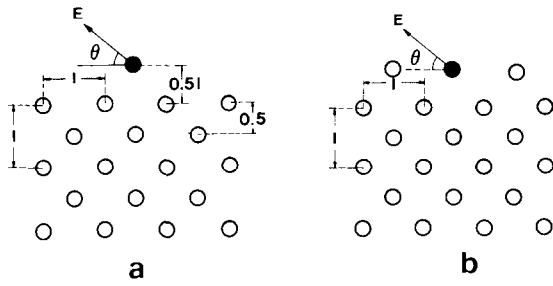
Fig. 1. The arrangement of the gold atoms in a 2D lattice for the dynamical calculation: (a) in the case of the surface adatom and (b) in the case of the in-surface atom.
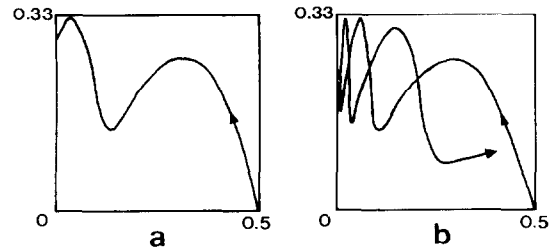

Fig. 2. The trajectories of an adatom: (a) when the atom just surmounts the surface barrier and (b) when the adatom is just reflected by the barrier in the case of fixing other atoms.

both cases the initial velocity from the Rutherford scattering was given to the blacked atoms only. The approximation of reducing a 3D problem to 2D is based on the assumption that the surface potential well has central symmetry. A fourth order of the Runge–Kutta method was employed for the numerical calculations and the dynamical calculation of the trajectories of adatom or in-surface atom were performed as a function of the energy and initial displacement direction of the surface atom. Of interest is the critical energy when the adatom or in-surface atom just surmounts the potential barrier built up by the neighboring atoms. Firstly all the other atoms were assumed fixed. Fig. 2 shows two typical trajectories of an adatom; in (a) when the surface atom just surmounts the surface barrier, and in (b) when the adatom is just reflected. Similar trajectories were obtained for the in-surface case. Figs. 3a and 3b show the critical curves of the energies for these situations; only atoms with kinetic energy

above the curve will diffuse. These two curves clearly show a smooth behavior with functionality no matter how complicated the trajectories of surface atoms. For the adatom, the critical curve has a simple parabolic character, while the critical curve of an in-surface atom appears more complicated. This is because for the in-surface case, the atom is strongly interacting with its four neighboring atoms.

Similar calculations for the case in which one neighboring atom is movable were also performed for both adatom and in-surface atom. Fig. 4a shows the case when the adatom is just reflected by the potential barrier, while fig. 4b shows it just surmounts. The neighboring atom vibrates around its equilibrium position in both cases. The calculations indicated that the time required for the ballistic diffusion process of one adatom or in-surface atom is around 10^{-13} s and the time required for kinetic energy of an adatom or in-surface atom to be transferred to its neighbors atoms is about 10^{-11}–10^{-12} s. The results showed
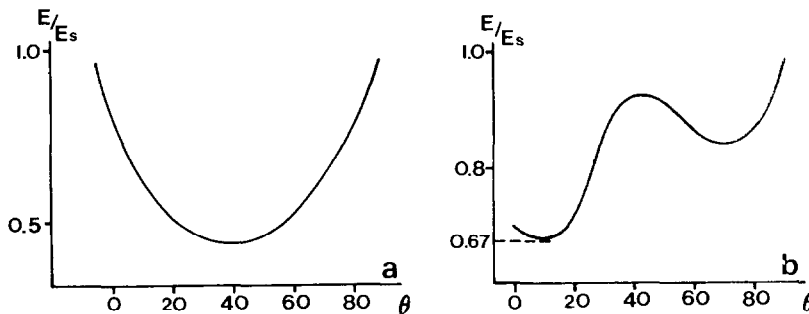

Fig. 3. The curves of the critical energy for the surface atom surmounting the surface potential barrier as the function of ejection angle of the excited atom: (a) in the case of adatom on the surface and (b) in the case of the in-surface atom.
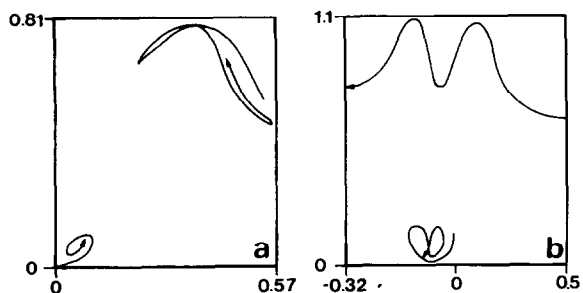
Fig. 4. The trajectories of an adatom in the case that one neighboring atom is movable: (a) when the adatom is just reflected by the surface barrier and (b) when the adatom just surmounts the surface barrier.

Fig. 5. The scattering geometry between the incident high energy electron and the surface atom.

no big change in the critical curve, and the assumption that the neighboring atoms are fixed appears to be a reasonable approximation.

For the scattering process we applied Rutherford scattering theory using the scattering geometry shown in fig. 5. The energy transferred to a single surface atom by a single scattered electron is given by the equation

$$E = E_m \cos^2(\theta'),\tag{1}$$

where E_m is the maximum energy that the electron can transform to the atom, which is related to the incident energy of the electrons as:

$$E_m = 2E_e(E_e + 2mc^2)/Mc^2,\tag{2}$$

where E_e is the incident energy, m the mass of the electron and M the mass of the adatom. Substitut-
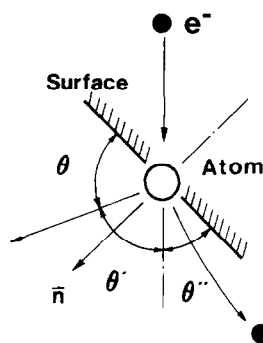
ing (1) into the equation for the critical curve,

$$f(\theta) = E/E_s,\tag{3}$$

we then obtain the following relationship

$$E_m/E_s = f(\theta)/\cos(180° - \theta'' - \theta).\tag{4}$$

Different values of θ'' represent different geometries of the surface with respect to the direction of the incident electron. The physical significance of eq. (4) is that the energy required for the diffusion of a surface atom is a function of the ejection angle θ and the angle between the surface and beam direction θ''. Plotting E_m/E_s versus θ for different θ'', we obtain a series of critical curves for E_m as shown in figs. 6a and 6b for the adatom and in-surface atom cases, respectively.

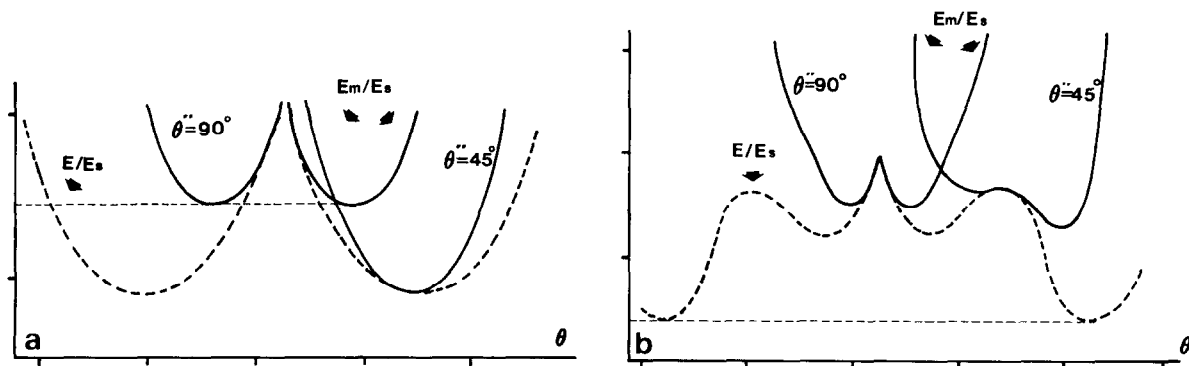These curves were then used to determine the scattering angle range within which the scattered

Fig. 6. The curves of the minimum incident energy required for diffusing: (a) an adatom and (b) an in-surface atom as the function of the ejection angle of the atom for the different angles between the surface and the incident momentum.
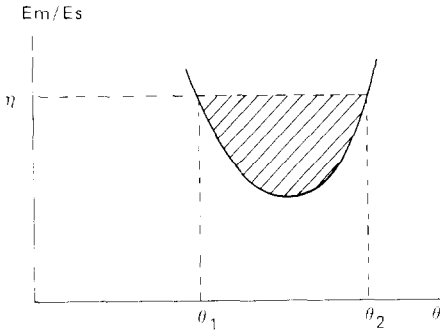
Fig. 7. The illustration of determining the diffusible angle range $\theta_1 - \theta_2$.

atoms can be diffused as shown in fig. 7. η is the value of E_m/E_s for the given accelerating voltage. The scattering probability of the adatom or in-surface atom is then given by

$$M_a = \int_\Omega \sigma(\theta) n_e \, d\Omega(\theta),\tag{5}$$

where the physical significance of M_a is the probability of one surface atom being scattered into a solid angle Ω per incident electron per second, $\sigma(\theta)$ is the differential Rutherford scattering cross-section, n is the electron flux, and Ω is the solid angle within which we are counting scattered surface atoms. If we substitute all relations with respect to angle for the quantities in (5), we obtain:

$$M_a = 4\pi n_e \left(\frac{ZZ'e}{2\mu v^2}\right)^2 \int_{\theta_1}^{\theta_2} |\sin(\theta'' + \theta)|$$

$$\times \left[1 + \left(1 + \frac{\sin^2 2(\theta'' + \theta)}{[m/M - \cos^2(\theta'' + \theta)]^2}\right)^{-1/2}\right]^{-2} d\theta,\tag{6}$$

where Z is the atomic number of the surface atom after modification for Coulomb screening, $Z' = 1$ for an electron, m is the reduced mass and v the relativistic velocity of electron; M is the mass of the adatom. The inverse of M_a, $T_a = 1/M_a$, has units of (atom · s/ST). Its physical significance is the time required for all atoms in a monolayer to diffuse. The upper and lower limits, θ_1 and θ_2, are determined by the value of E_m which was calculated from the kinetic energy of the incident electrons.

3. Results

To provide some hard data, we have taken an accelerating voltage of 200 keV and a current density of 1.8 A cm. The calculated results for different surface geometries for both adatom case and in-surface case are shown in table 1. They indicate that the time required for scattering of one monolayer is about several hundred seconds for this specific voltage and metal. (Note that this value should be compared with the intrinsic thermal diffusion of the surface which we would expect to be in general far faster.) The time for profile imaging position $\theta'' = 0$ is longer than that for other positions, indicating that the profile imaging technique is less influenced by ballistic damage. In general terms, T_a is inversely proportional to the square of atomic number Z, i.e. the heavier the atom, the shorter the "sitting time" T_a. T_a is also related to the cohesive energy E_s, and larger cohesive energies make the critical curve steeper and reduce the diffusible angular range, and therefore increase T_a. The influence of the energy of incident electrons on T_a is shown in two ways. At higher energies the relativistic electron

Table 1

θ'' (deg)	$\theta_1 - \theta_2$ (rad)		$M_a \times 10^{-3}$ (ST/atom·s)		T_a (atom·s/ST)	
	Adatom	In-surface	Adatom	In-surface	Adatom	In-surface
90	0.75–2.35	1.20–1.90	13.88	1.48	72	675
75	1.71–2.58	1.60–2.10	5.55	0.71	180	1401
45	1.82–2.96	2.07–2.95	4.88	3.04	205	329
0	2.45–3.10	2.70–3.14	4.23	1.26	236	793

velocity v increases, reducing the cross section for scattering and therefore increasing T_a; but it also makes the diffusible angle range $\theta_1-\theta_2$ wider, which reduces T_a. To some extent these two effects offset each other. At low energy ($V_e < 300$ kV), the velocity dominates, and the time required for the diffusion of one monolayer increases with accelerating voltage. A higher energies the velocity does not increase so fast (due to relativistic effects) and the diffusible range effect will dominate.

4. Discussion and conclusion

Our results indicate that ballistic surface diffusion is strongly dependent upon the properties of materials. There exists a threshold voltage for the ballistic surface diffusion which for Au is about 135 kV. We encounter a problem when we attempt to reconcile these results with some experimental data on the surface sputtering threshold for gold obtained by Cherns et al. [24]. These authors obtained a value of 459 kV. At this voltage the maximum energy transferred to an atom is 7.22 eV which is approximately twice the cohesive energy. There are two possible reasons for this discrepancy. First, there may have been a contamination layer in the experiments, so that the "sputtering threshold" might in fact represent the threshold to sputter gold through a 20 Å carbon contamination layer. Alternatively 459 kV may represent the threshold for high yield due to a more complicated multi-atom sputtering process, rather than threshold of simple sputtering. It seems quite likely that there may (at higher voltages) be more complicated and damaging processes, both for sputtering and for athermal diffusion. It would clearly be of interest to see the results of careful electron microscope imaging work at different temperatures.

A feature of the results to note is that the surface geometry has a strong effect on ballistic diffusion; and the ballistic diffusion on profile surfaces appears to be the smallest, whereas the

prospect is clearly not so good for plan view imaging, particularly of the exit surface of specimens where we can expect fairly severe damage.

Acknowledgements

References

[1] N. Osakabe, Y. Tanishiro, K. Yagi and G. Honjo, Surface Sci. 102 (1980) 424.
[2] T. Hsu and J.M. Cowley, Ultramicroscopy 11 (1983) 239.
[3] Y. Uchida, G. Lehmpfuhl and J. Jäger, Ultramicroscopy 15 (1984) 119.
[4] N. Shimizu, Y. Tanishiro, K. Kobayashi, K. Takayanagi and K. Yagi, Ultramicroscopy 18 (1985) 453.
[5] L.D. Marks and D.J. Smith, Nature 303 (1983) 316.
[6] L.D. Marks, Phys. Letters 51 (1983) 1000.
[7] L.D. Marks, V, Heine and D.J. Smith, Phys. Rev. Letters 52 (1984) 656.
[8] L.D. Marks, Surface Sci. 139 (1984) 281.
[9] A.J. Forty, Contemp. Phys. 24 (1983) 271.
[10] K. Takayanagi and K. Yagi, Trans. Japan Inst. Metals 24 (1983) 337.
[11] R.L. Heines, Thin Solid Films 35 (1976) 229.
[12] D. Cherns, Phil. Mag. 30 (1974), 549.
[13] J.C. Bourgoin and J.W. Corbett, Phys. Letters A38 (1972) 135.
[14] D. Luzzi, PhD Thesis, Northwestern University, USA (1986) p. 269.
[15] S.B. Fisher, Radiation Effects 5 (1970) 239.
[16] L.D. Marks, A.K. Petford and M. O'Keeffe, in: Proc. 43rd Annual EMSA Meeting, Louisville, KY, 1985, Ed. G.W. Bailey (San Francisco Press, San Francisco, 1985) p. 265.
[17] A.K. Petford, L.D. Marks and M. O'Keeffe, Surface Sci. 172 (1986) 496.
[18] Peter J. Feibelman and M.L. Knotek, Phys. Rev. B18 (1978) 6537.
[19] D. Menzel and R. Gomez, J. Chem. Phys. 40 (1964) 1164.
[20] M.L. Knotek and P.J. Fcibelman, Phys. Rev. Letters 40 (1978) 964.
[21] M.L. Knotek, Phys. Scripta 16 (1983) 94.
[22] M.L. Knotek, Phys. Today (September 1984) 27.
[23] J.D. Doll and H.K. McDowell, J. Chem. Phys. 77 (1982) 479.
[24] D. Chern, M.W. Finnis and M.D. Mathews, Phil. Mag. 35 (1977) 135.